

Chemical state of nitrogen and visible surface and Schottky barrier driven photo-activities of N-doped TiO₂ thin films

Journal:	<i>The Journal of Physical Chemistry</i>
Manuscript ID:	jp-2009-024816.R1
Manuscript Type:	Article
Date Submitted by the Author:	27-May-2009
Complete List of Authors:	Romero-Gomez, Pablo; Instituto de Ciencia de Materiales de Sevilla, Superficies, Interfases y Capas Finas Rico, Victor R.; Instituto de Ciencia de Materiales de Sevilla, Superficies, Interfases y Capas Finas Borras, Ana; CSIC-Univ. Sevilla, ICMSE Barranco, Angel; Instituto de Ciencia de Materiales de Sevilla, Superficies, Interfases y Capas Finas; Instituto de Ciencia de Materiales de Sevilla, Surfaces Interfaces and Thin Films Espinós, Juan P.; Instituto de Ciencia de Materiales de Sevilla, Superficies, Interfases y Capas Finas Cotrino, Jose; Instituto de Ciencia de Materiales de Sevilla, Superficies, Interfases y Capas Finas; Universidad de Sevilla, Instituto de Ciencia de Materiales Gonzalez-Elipe, Agustín; Instituto de Ciencia de Materiales de Sevilla (CSIC-Univ. Sevilla), Superficies, Interfases y Capas Finas



1
2
3 **Chemical state of nitrogen and visible surface and Schottky barrier driven photo-**
4 **activities of N-doped TiO₂ thin films**
5
6
7

8 P. Romero- Gómez¹, V. Rico¹, A. Borrás, A. Barranco¹, J.P. Espinós¹, J. Cotrino^{1,2},
9 A.R. González-Elipe^{1*}

10 *1. Instituto de Ciencia de Materiales de Sevilla (CSIC-Univ. Sevilla). Avda. Américo*
11 *Vespucio 49. 41092 Sevilla (Spain). <http://www.sincaf-icmse.es>*

12 *2. Departamento de Física Atómica, Molecular y Nuclear. Universidad de Sevilla.*
13 *Avda. Reina Mercedes 49, 41012 Sevilla. Spain.*

14
15
16
17
18
19
20
21 *arge@icmse.csic.es
22

23
24 **Abstract**
25

26 N-doped TiO₂ thin films have been prepared by plasma enhanced chemical vapour
27 deposition (PECVD) and by physical vapour deposition (PVD) by adding nitrogen or
28 ammonia to the gas phase. Different sets of N-doped TiO₂ thin films have been obtained
29 by changing the preparation conditions during the deposition. The samples have been
30 characterized by X-ray diffraction (XRD), Raman, UV-vis. spectroscopy and X-ray
31 photoemission spectroscopy (XPS). By changing the preparation conditions different
32 structures, microstructures, and degrees and types of doping have been obtained and
33 some relationships established between these film properties and their **visible light**
34 **photoactivity**. The N1s XP spectra of the samples is characterized by three main
35 features, one tentatively attributed to Ti-N (i.e. nitride with a BE of 396.1) and two
36 others with BEs of 399.3 and 400.7, tentatively attributed to nitrogen bonded
37 simultaneously to titanium and oxygen atoms (i.e. Ti-N-O like species). By controlling
38 the deposition conditions it is possible to prepare samples with only one of these species
39 as majority component. It has been shown that only the samples with Ti-N-O like
40 species show surface photoactivity being able to change its wetting angle when they are
41 illuminated with visible light. The presence of these species and an additional complex
42 structure formed by a mixture of anatase and rutile phases is an additional condition that
43 is fulfilled by the thin films that also present photo-catalytic activity with visible light
44 (i.e., **surface and Schottky barrier driven photoactivities**). The relationships existing
45 between the reduction state of the samples and the formation of Ti-N or Ti-N-O like
46 species are also discussed.
47
48
49
50
51
52
53
54
55
56
57
58
59
60

1. Introduction

The quest for N-doped TiO₂ thin films and powders was fostered by the discovery of Ashahi et al.¹ that titanium dioxide may become photo-active when irradiated with visible light. Since the publication of this seminal work much effort has been dedicated to both the development of different experimental strategies of doping²⁻⁷ and the understanding of the reasons that make this material photo-active in the visible when appropriately doped.^{8,9} However, none of these two questions has yet a clear answer and some controversy exists because the obtained results are not always reproducible. This situation is well reflected in recent reviews dealing with this subject.^{10,11}

From an experimental point of view, X-ray photoemission spectroscopy (XPS) has been the most widely used technique to check the state of nitrogen in N-doped TiO₂ materials. Already Ashahi et al.¹ pointed out that there were at least two types of nitrogen species in their N-doped TiO₂. A first one was characterized by a binding energy (BE) of about 396 eV (hereafter called α) and another one by a BE of about 400 eV (hereafter called β). These two species have been determined by XPS with different total and relative intensities in other N-doped TiO₂ materials.^{1, 6, 7, 12-16} However, no agreement exists about the assignment of these nitrogen species that have been alternatively attributed to nitride,^{1, 7, 12} NH,⁷ molecular nitrogen^{7, 16} or NO^{7, 14} species, either in substitutional or interstitial locations of the TiO₂ lattice.

N-doped TiO₂ has been prepared in the form of powder or as thin films. In this latter case magnetron sputtering,^{5, 17, 18} electron beam evaporation,¹⁹ ion beam assisted deposition (IBAD)²⁰ or plasma enhanced chemical vapour deposition (PECVD)²¹ have been utilized. The photoactivity of N-doped TiO₂ thin films can be checked by looking to its photocatalytic ability to produce chemical reactions under the action of light and/or by following the evolution of the wetting angle of water or other liquids on its surface as a function of the irradiation time. As justified in the discussion, we will refer to these two types of photo-activity as *surface* and *Schottky barrier driven* photo-activities, respectively. In some works in the literature, the two effects have been implicitly taken as equivalent. However, this assumption must be considered critically as even for un-doped TiO₂ it has been demonstrated that the efficiencies for photocatalytic degradation of dyes and the change in wetting angle upon UV light irradiation can be quite different.²² In this line, we have recently shown that TiO₂ thin films doped by nitrogen ion beam implantation become partially hydrophilic when irradiated with visible light, even if no photo-catalytic activity was observed for these samples.²³

1
2
3 The present paper addresses some of the aforementioned open issues by studying the
4 synthesis and analyzing the properties of N-doped TiO₂ thin films prepared by PECVD
5 and physical vapour deposition (PVD) at glancing angle evaporation. The plasma and
6 evaporation conditions have been changed in order to control the doping state, the type
7 of species present in the samples and other properties of the films. In particular, we have
8 tried to correlate the type of species formed in each case with the observed *surface* and
9 *Schottky barrier driven* photo-activities of the samples. **This latter** has been checked by
10 following the *photo-catalytic degradation* of dyes in aqueous solutions. For the purpose
11 of controlling the state and amount of nitrogen into the films, the composition (i.e.
12 nitrogen, oxygen or hydrogen content) and other characteristics of the plasma used for
13 decomposition of the precursors during PECVD have been systematically changed. In
14 addition, the performance of films from a N-containing precursor (i.e., with Ti-N bonds
15 present in the precursor molecule) is compared with that of films deposited from an
16 standard isopropoxide precursor typically used for the fabrication of TiO₂ optical thin
17 films by PECVD. In this latter case, **N-doping of samples is produced by reaction with**
18 **nitrogen species** of the plasma discharge. By PVD, the residual gas during evaporation
19 and the temperature of the substrate have been critical parameters to get thin films with
20 *Schottky barrier driven* photo-activity in the visible. The films have been characterized
21 by Scanning Electron Microscopy (SEM), X-ray photoemission spectroscopy (XPS),
22 Raman spectroscopy, X-ray diffraction (XRD) and UV-visible absorption spectroscopy.
23 A critical evaluation of the different results obtained has enabled a first evaluation of the
24 influence of the state of nitrogen and other thin film characteristics as their structure and
25 microstructure for the visible activation of N-doped TiO₂.
26
27
28
29
30
31
32
33
34
35
36
37
38
39
40
41
42
43
44

45 **2.Experimental**

46 *2.1 Thin film preparation and selected samples*

47
48
49
50
51
52 A series of TiO₂ and N-doped TiO₂ thin films were prepared by PECVD in a plasma
53 reactor with a remote configuration. The system, supplied with a microwave plasma
54 source (SLAN, from Plasma Consult, GmbH, Germany) has been described in previous
55 works.^{24, 25} It consists of an external 2.45 GHz microwave electron cyclotron resonance
56 (MW-ECR) plasma source coupled to the reaction chamber and separated from it by a
57 grid to avoid the microwave heating of the substrates. Under normal conditions of
58
59
60

1
2
3 operation, the grid confines the plasma out of the reaction chamber (remote plasma
4 conditions) where the substrate and the precursor dispenser are located. Ion
5 bombardment effects on the growing sample can be enhanced by externally applying a
6 voltage bias to the substrate or by decreasing the operation pressure of the plasma.
7 Control of this effect has demonstrated to be quite effective in modifying the samples
8 characteristics (structure, microstructure), even if the plasma composition remains the
9 same. Titanium tetra-isopropoxide (TTIP) was used as titanium precursor. For
10 comparison, some experiments were also carried out with the nitrogen- containing
11 Tetrakis(diethylamido)titanium(IV) (TDEAT) precursor. Scheme 1 shows a
12 representation of the two precursors used in this work. It is worth noting the four direct
13 Ti-N bonds existing in the TDEAT.

14
15
16
17
18
19
20
21
22
23
24 The plasma source was operated with a power of 400 W with either pure O₂, O₂ + Ar or
25 mixtures of gases containing nitrogen, basically N₂+O₂ and N₂+H₂+O₂. The synthesis of
26 the films was carried out at variable temperatures between room temperature and 523 K,
27 although only results at 298 and 523 K are reported. For dosing TTIP or TDEAT in a
28 controlled way they were placed in a stainless steel recipient through which oxygen was
29 bubbled while heating at 305 K. Both the bubbling line and the shower-type dispenser
30 used to dose the precursor into the chamber were heated at 373K to prevent any
31 condensation in the tube walls. Total pressure during deposition was 4x10⁻³ Torr
32 (normal operation conditions). Another series of samples was prepared at a much lower
33 pressure (4x10⁻⁴ Torr) with N₂ +O₂ as plasma gas. In this latter case, the system was
34 working under the typical ECR conditions characterized by a higher ion density than at
35 higher pressures.²⁶ A deposition rate of approximately 2.5 nm min⁻¹ was estimated by
36 means of a quartz crystal monitor for the samples grown at room temperature.

37
38
39
40
41
42
43
44
45
46
47
48 Although we prepared a large number of PECVD samples by changing synthesis
49 parameters such as temperature of substrate, pressure, voltage bias applied to the
50 substrate and mixture of plasma gases, we have summarized the results by referring to
51 the type of nitrogen species detected by XPS. Some basic properties of the set of
52 samples selected for this analysis have been gathered in Table 1, where details about
53 some relevant parameters of the procedure of synthesis are indicated for samples
54 prepared with TTIP as precursor. Occasionally, comments are also made in the text to
55 samples prepared by modifying the preparation parameters reported in Table 1. The
56
57
58
59
60

1
2
3 order A-E defined in this table has been established after the relative N/Ti ratio
4 **determined by XPS** as reported in the next section. It can be realized that the thin films
5 were prepared at 298 K (samples C) or 523 K (samples A, B, D, E), by using mixtures
6 of **O₂+N₂ that can be rich either** in O₂ (samples A) **or in** N₂ (samples B, C and E) or also
7 contain H₂ (samples D). A bias voltage of 150 V was applied to the substrate for the
8 majority of the preparations reported in Table 1 (samples B-E). In one case, ECR low
9 pressure conditions were also used for the deposition of the films (sample E). An un-
10 doped TiO₂ sample (sample REF), intended as a reference, was prepared with pure
11 oxygen as plasma **gas**. A fully account of the characteristics of this reference thin film
12 can be found in previous publications.^{24, 25} From these previous works, an important
13 feature of the un-doped TiO₂ thin films prepared by PECVD is that they are amorphous
14 when prepared at T<523 K, but become crystalline when prepared at 523 K as
15 temperature of the substrate.

16
17 Another series of N-doped TiO₂ thin films were prepared by PVD at glancing angles
18 (i.e., GAPVD).²⁷⁻²⁹ The films studied in the present paper were prepared by electron
19 evaporation of TiO₂ as target material and an evaporation angle of 85° between the
20 substrate and the evaporation **source**. During evaporation, the substrate was kept at 673
21 K, while a 50% mixture of NH₃+O₂ at a pressure of 10⁻⁴ torr was dosed in the
22 evaporation chamber. This type of thin films **is** labelled as sample F. Some of **its** basic
23 properties are also summarized in Table 1. It is important to indicate that, **in a similar**
24 **way than the PECVD samples**, other films prepared by PVD using different deposition
25 conditions **with nitrogen as the sole residual gas** only showed *surface* photo-activity and
26 will not be considered specifically here.

27
28 All the films were deposited simultaneously on a silicon wafer and on quartz plates.
29 Thickness of the prepared samples was estimated by measuring the mass thickness of
30 the films by both X-ray fluorescence (XRF) and Rutherford Back Scattering (RBS).
31 Note that the mass thickness is different than the actual thickness of the films
32 determined by Scanning Electron Microscopy and/or by optical methods. Typical
33 (optical) thicknesses of the thin films prepared on silicon or on fused silica substrates
34 were in the order of 300 nm. However, for SEM cross section views, thicker films were
35 prepared on silicon substrates.

36 37 38 39 40 41 42 43 44 45 46 47 48 49 50 51 52 53 54 55 56 57 58 59 60 *2.2 Methods of characterization*

1
2
3 The optical properties of the samples were determined by UV-vis absorption
4 spectroscopy (Perkin-Elmer Lambda 12 Spectrometer) for samples prepared on fused
5 silica. Typical thickness of the samples used for optical characterization was around 350
6 nm.
7
8

9
10 XPS spectra of the films were recorded on an ESCALAB 210 spectrometer working
11 under energy transmission constant conditions. The Mg K α line was used for excitation
12 of the spectra. They were calibrated in binding energy (BE) by referencing to the C1s
13 peak due to contamination taken at 284.6 eV. Quantification was done by calculating
14 the area of the peaks and by correcting then with the sensitivity factor of each
15 element/electronic level. To remove the carbon and other contamination from the
16 surface of the films, they were subjected to a gentle sputtering with Ar⁺ ions of 2.5 keV.
17 A current density of about 10 $\mu\text{A cm}^{-2}$ for a sputtering time of 5 min was used in these
18 treatments. Fitting analysis of the N1s peak was carried out by using elemental bands of
19 [gaussian/lorentzian](#) shape after background subtraction of the spectra with a Shirley-
20 type curve.
21
22

23 SEM cross section and normal images were measured in a Hitachi S5200 field emission
24 microscope for thin films grown on a silicon wafer. The thickness of the samples for
25 SEM analysis was generally higher than for the other characterization experiments.
26
27

28 Structural characterization of the thin films was done by X-ray Diffraction in a Siemens
29 D5000 diffractometer.
30
31

32 Raman spectra were collected in a LabRAM HR High Resolution 800 UV Confocal
33 Raman Microscope. For the measurements a green laser (He-Ne 532.14 nm), 600
34 line/mm, 100X objective, 20 mW and 100 μ pinhole, was used.
35
36

37 Measurement of the surface electrical conductivity of the samples was carried out with
38 the typical four point probe test. A Keithley 617 Electrometer and a Hewlett-Packard
39 34401 A Voltammeter were used for the measurements. These consisted of applying a
40 voltage ranging between -0.25 and 0.25 V to the two external probes and the
41 measurement of the current flowing between the two internal probes.
42
43

44 Measurement of contact angle was carried out by the Young method by dosing small
45 droplets of deionized and bidistilled water on the surface of the illuminated samples. In
46 the experiments where the contact angle variation was determined as a function of the
47 illumination time, a metal foil acting as a shutter was used to close and open the lamp
48 output. All wetting angle measurements within a given experiment were taken after
49 illumination for successive periods of time. Therefore, the time scale in the plots refers
50
51
52
53
54
55
56
57
58
59
60

1
2
3 to the accumulative illumination of the samples. The maximum uncertainty in the
4 determination of the water contact angle is about 10° depending on the sample position.
5 In the course of this investigation it was noticed that the “as-prepared” thin films were
6 more hydrophilic than the same samples a given time after their preparation. Therefore,
7 the reported results correspond to samples that were stored in a desiccator, at least for
8 two months, before testing their photo-activity.
9

10 Illumination of the samples was carried out with a Xe discharge lamp with a photon
11 intensity at the position of the samples of 2 Wcm^{-2} for the complete spectrum of the
12 lamp. For simplicity we will refer this situation in the text and figures as UV
13 illumination. Other experiments consisted of the illumination with the same lamp by
14 placing an UV filter (i.e., $\lambda > 400 \text{ nm}$) between the lamp and the sample. The light
15 intensity was then 1.6 Wcm^{-2} at the sample position. In all cases an infrared filter (i.e., a
16 water bath) was kept between the lamp and the samples to prevent any possible heating
17 by the infrared radiation.
18

19 Photocatalytic tests were carried out in a specially constructed experimental setup. It
20 consisted of a small cell made of quartz (total volume 3 cm^3) where 2 cm^3 of a 3.5×10^{-5}
21 M solution of methyl orange dye was placed together with a piece of a silicon substrate
22 ($1 \times 0.8 \text{ cm}^2$) with the thin film deposited on its surface. The films, deposited on a silicon
23 wafer, were irradiated from a frontal position while spectra of the solution were
24 simultaneously recorded with the help of two optical fibres connected to an UV-visible
25 spectrometer and placed in opposite sides of the vessel. The solution was bubbled with
26 oxygen and the vessel closed with a Teflon cover to avoid the evaporation of the liquid.
27 The whole set-up was refrigerated with a fan placed behind the vessel. This
28 experimental set-up permitted the automatic recording of the spectra from the solution
29 while the films are irradiated. Blank experiments were also carried by placing a piece of
30 a silicon wafer without any TiO_2 thin film deposited on its surface. The intensity of the
31 UV+vis radiation at the position of the cell was 1.8 W (i.e., approximately 0.3 Wcm^{-2}
32 for photons with $\lambda < 380 \text{ nm}$). Visible illumination was carried out by placing a filter
33 (i.e., $\lambda > 380 \text{ nm}$) between the Xe discharge lamp and the reaction vessel. The intensity
34 of the visible radiation at the cell position was 160 mW cm^{-2} . Since the illumination
35 area of the samples was defined with a slit of 1 cm^2 and was always the same for all the
36 experiments, their results can be properly compared. The curves reported in the paper to
37 show the evolution of the concentration of dye versus illumination time have been
38 obtained after dividing the curves obtained with the thin films by the curve of the blank
39
40
41
42
43
44
45
46
47
48
49
50
51
52
53
54
55
56
57
58
59
60

1
2
3 experiment. We must stress that placing a silicon wafer in the blank experiment is
4 critical for a proper correction of the results. In fact, in the absence of any reflecting
5 surface in the cell, the effect of the reflected light [through the solution](#) is not considered
6 [in the blank experiment](#) and flawed final results are obtained.
7
8
9

10 11 12 **1. Results**

13 *3.1. Microstructure and structure of the thin films*

14 Fig. 1 shows a series of SEM micrographs corresponding to samples A-F and to the
15 reference sample. It is apparent from this figure that the films prepared at 298 K ([i.e.](#)
16 [sample C](#)) or at 523 K under ECR conditions ([i.e., sample E, the image of this latter not](#)
17 [shown](#)) present a homogenous microstructure where no columns or crystals can be seen.
18 A similar microstructure was always obtained under normal pressure conditions of
19 PECVD by applying a high bias voltage to the substrate (*i.e.* voltages of the order of
20 300V, image not shown). This result [and the homogenous microstructure of sample E](#)
21 [support that an enhancement of the ion bombardment effects during the film growth](#)
22 [favour the surface mobility of the ad-species during growth and, as a result, a](#)
23 [homogeneization of the microstructure](#). This contrasts with the microstructure of the
24 films prepared under “normal” PECVD conditions ([i.e., samples A,B and D](#)) at 523 K
25 as substrate temperature and 150 V as bias voltage, all of them presenting a columnar
26 microstructure formed by the agglomeration of small grains and/or crystallites quite
27 similar to those of the reference sample. The microstructure of sample F prepared by
28 PVD at glancing angles was characterized by tilted columns that leave large open pores
29 between them. This microstructure is typical of this kind of thin films.²⁹ A rough
30 estimation of the porosity of these films based on the assessment of their refraction
31 indices yields values of the order of 40% of void spaces.
32
33
34
35
36
37
38
39
40
41
42
43
44
45
46
47
48

49 The structure of the films was analysed by XRD. The films prepared at 298 K (*i.e.*
50 [samples C](#)) were all amorphous, while those prepared by PECVD at $T > 523$ K ([i.e.,](#)
51 [samples A, B, D and E](#)) were amorphous or crystalline depending on the particular
52 experimental protocol used in each case. Fig. 2 reports a series of diffraction diagrams
53 recorded for various samples. The diagrams in this plot corresponding to samples A and
54 B are typical of the anatase structure of TiO_2 although the relative intensity of the
55 different peaks of the diagram slightly differs from that of a polycrystalline sample
56 where the crystals are randomly oriented (see the patterns of anatase and rutile included
57
58
59
60

1
2
3 in the figure for comparison). The crystal size determined by the Scherrer method for
4 the set of samples A and B yielded values of 84.2 and 85.0 nm, respectively. From the
5 (101) peak of the anatase phase of the REF sample, a crystal size of 89.2 nm could be
6 also determined. Samples C, D and E were amorphous, at least as determined by XRD.
7 This result was quite surprising since samples D and E were prepared by PECVD at 523
8 K, the temperature at which anatase films are obtained by this method when using an
9 oxygen plasma.²⁴ Some of these sample characteristics are collected in Table 1. It is
10 also worth noting that a thin film prepared under conditions similar to those of thin
11 films B, but by biasing the substrate with a voltage of 300 V, was also amorphous.

12 The diagram of samples F prepared by GAPVD, also reported in Fig. 2, was
13 characterized by a rich structure where peaks of anatase and rutile can be detected. The
14 crystal size of the anatase phase was estimated in 22.6 nm and that of rutile in 9 nm.

15 A deeper insight into the structure of the films can be obtained by Raman spectroscopy.
16 Fig. 3 (top) shows the Raman spectra of samples A-F compared with the spectrum of
17 the reference sample in the region comprised between 210 and 800 cm^{-1} . These spectra
18 are characterized by a series of peaks with different intensities located at 395, 515 and
19 638 cm^{-1} .³⁰ Samples C and E have a very poor crystallinity as no resolved peaks of
20 anatase can be detected in this region of the spectra.

21 The Raman spectrum of samples F shows a more complex pattern where, *in agreement*
22 *with literature*,³¹ peaks at the positions of the anatase and rutile phases of TiO_2 can be
23 detected. This spectrum confirms the detection by XRD of these two phases.

24 It is worth stressing that no clear hints of an oxinitride phase could be found in the
25 previous spectra. The formation of this phase in N-doped TiO_2 thin films has been
26 claimed by some authors³² from the fitting analysis of Raman spectra very similar to
27 those of samples A or B in Fig. 3. Recently, other authors^{33, 34} have attributed the
28 background features appearing at around 328, 585, 680 and 815 cm^{-1} to defective
29 titanium oxide. *For* the case of thin films F, we think that the *peaks in Fig. 3 (top)*
30 *around these positions are due to spectral features* of the rutile phase detected by XRD.

31 Fig. 3 (bottom) shows an enlarged view around the region of the main peak of the
32 Raman spectrum of anatase attributed to the E_g vibration mode.³⁰ For samples A, B and
33 F and even more pronounced for sample D, the position of the main mode at around 150
34 cm^{-1} is shifted from 143.2 cm^{-1} in the reference anatase to around 150.0 cm^{-1} and
35 beyond in samples A, B, F and D. In these four cases, the peak also *broadens* with
36 respect to the peak of the reference sample. It is important to remark that for sample D

1
2
3 no well resolved diffraction peaks could be observed by XRD, thus sustaining that
4 Raman can be a more sensitive technique to detect first crystallization stages in thin
5 films. Frequency shift and line width broadening of the main mode have been attributed
6 to crystalline size effects³²⁻³⁴ and/or to the accumulation of structural defects and/or
7 lack of stoichiometry of the oxide.³⁵ Since the cristal size determined by XRD is not
8 much smaller in samples A and B (although it is smaller in sample and F) than in the
9 REF sample we must conclude that accumulation of structural defects and/or some
10 chemical reduction with a loose of stoichiometry are likely the main reasons for the
11 observed Raman shift in these samples.
12
13
14
15
16
17
18
19
20

21 3.2. UV-vis spectra and reduction degree of the films

22 A first assessment of the reduction state of the oxide thin films was obtained by
23 measuring their surface conductivity. Samples A, B, C and F present a high surface
24 resistivity and no reliable final data on sheet resistance could be obtained with the used
25 technique. However, surface conductivity in the dark could be measured for samples D
26 and E. Sample E was the most conductive one with an estimated resistivity of 1.5×10^{-1}
27 (cm Ω). The measured values were dependent on the time elapsed since the preparation
28 of the samples, the conductivity slightly decreasing for the sample stored for long
29 periods of time. Surface conductivity in titanium oxide thin films is associated with the
30 presence of vacancies and other structural defects within a layer of several tenths of
31 nanometer, indicating a certain lost of stoichiometry (i.e., formation of Ti^{3+} species).³⁶
32 Fig. 4 shows the UV-vis absorption spectra of samples A-F, together with the spectrum
33 of the anatase thin film taken as a reference. The value of the absorption edges,
34 obtained by the Tauc method by extrapolating to zero the function $A(h\nu)^{1/2}$,³⁷ is
35 reported in Table 1. The obtained data indicate that samples A and C present absorption
36 edges which are very close to that of the reference anatase film, while samples B, D, E
37 and F present absorption edges which are shifted to smaller energies. In addition,
38 samples B, D, E and F present some specific absorption features in the blue region of
39 the spectra that are clearly distinguishable from the typical interference oscillations
40 presented by high refractive index thin films deposited on a quartz substrate. For
41 samples B, D and F, this first absorption feature is located around 420 nm. In samples
42 E, besides an absorption around this wavelength, there is also a broad absorption
43 extending through the whole range of wavelengths and centred at $\lambda > 500$ nm. Very
44 likely this broad absorption is related with the existence of a high concentration of
45
46
47
48
49
50
51
52
53
54
55
56
57
58
59
60

1
2
3 structural defects and/or Ti^{3+} species as it can be deduced from the relatively high
4 surface conductivity of this sample.

5
6 The absorption spectra of N-doped titanium oxide has conceited much interest in
7 literature because absorption features in the visible have been taken as a hint of visible
8 photo-activity of this material and because of a vivid controversy about the effect of
9 doping in narrowing the band gap of TiO_2 .^{10, 11} According to Serpone et al.³⁸
10 absorption features appearing in the visible in anion doped titanium oxide originate
11 from colour centres associated with the reduction of the titanium oxide rather than with
12 a narrowing of the band gap as claimed by others.³⁹⁻⁴¹ Meanwhile, Lin et al.,⁴²
13 combining theoretical calculations with the analysis of UV-visible spectra, concluded
14 that the optical absorption of N-doped TiO_2 is primarily located between 400 and 500
15 nm, while that of oxygen-deficient TiO_2 appears above 500 nm. These authors coincide
16 in that no narrowing of the band gap of TiO_2 occurs as an effect of the incorporation of
17 nitrogen into the structure of the oxide. In relation with our results, we can tentatively
18 assume that samples E, depicting a broad absorption at $\lambda > 500$ nm and showing a
19 measurable surface conductivity, is chemically reduced and presents a considerable
20 concentration of oxygen vacancies and other defects in its structure. Meanwhile, the
21 absorption features at around 430 nm found in samples B, D and F are likely related
22 with absorption centres associated to nitrogen incorporated within the structure of the
23 titanium oxide.

3.3 XPS analysis and chemical state of nitrogen

24
25
26
27
28
29
30
31
32
33
34
35
36
37
38
39
40
41
42 XPS has been used to check whether nitrogen has been incorporated within the structure
43 of the titanium oxide films. This technique provides also information about the actual
44 chemical state of nitrogen in the different samples. Fig. 5 shows N1s fitted
45 photoemission spectra recorded for samples A-F. The spectra are represented by
46 applying different multiplication factors to bring all the spectra to a similar height. The
47 N/Ti ratios determined for these samples are reported in Table 1. The obtained data
48 show that samples C, D and E have a high content of N, while in samples A and B this
49 amount approximately decreases by one order of magnitude. Sample F presents a
50 spectrum that is similar to that of sample A. To a first approximation, the N1s spectra in
51 Fig. 6 can be considered as the contribution of three main components, a first one
52 centred around 396 eV (species α) and two others centred around 400 eV (species β and
53 β'). Photoemission spectra of the O1s, C1s and Ti2p levels were also recorded. The
54
55
56
57
58
59
60

1
2
3 O1s and Ti2p spectral shapes were quite similar in all cases and equivalent to the
4 reported spectra of TiO₂ (i.e., attributed to O⁻ and Ti⁴⁺ species⁴³). The corresponding
5 spectra are reported in the supporting information S1. The C1s spectra was
6 characterized by a main peak at 284.6 eV, taken as a reference for the BE scale of the
7 spectra. In some cases a small shoulder at about 290 eV could be observed in the
8 spectra. This peak is normally attributed to carbonate species,⁴⁴ while the main peak is
9 ascribed to carbonaceous rests contaminating the surface of the samples. For the
10 PECVD samples, another source of this spurious carbon can be some adsorbed rests of
11 the organic parts of the titanium precursor. The amount of contaminating carbon (i.e.,
12 around 15% atomic) was similar to that detected in other oxide thin films handled in air.
13 Its surface character was confirmed by subjecting the examined thin films to a mild
14 sputtering treatment for 5 min (see the experimental part). After this treatment the
15 carbon content in the samples decreased to less than 7 % atomic in all cases. This
16 contrasts with the fact that the N/Ti ratios measured for the sputtered films remained
17 almost unmodified after that treatment. This supports that nitrogen is distributed
18 homogeneously through all the films. Apart from a broadening in the spectral shape, the
19 form of the N1s spectra in the different samples was not modified significantly after that
20 treatment (see supporting information S1). This indicates that the different species
21 identified in the spectra of Fig. 5 distribute homogeneously through the first layers of
22 the films. It is also interesting that in sample E subjected to the sputtering treatment, the
23 Ti2p level depicted a shoulder at 456.5 eV that can be attributed to Ti³⁺ species. Since in
24 the other samples, such a feature is not so clearly observed (note that TiO₂ is always
25 reduced when subjected to Ar⁺ sputtering due to the preferential loss of oxygen⁴⁵). This
26 result sustains the previous evidences in section 3.2 in the sense that this sample is
27 partially reduced.

28
29
30
31
32
33
34
35
36
37
38
39
40
41
42
43
44
45
46
47
48 In relation with the XPS analysis of samples, it is also important to remark that,
49 particularly for samples D and E and to lesser extent B, the spectra underwent a certain
50 evolution with time. This evolution is characterized by a relative decrease in the α band
51 at 396 eV and an increase in the intensity of the β bands around 400 eV.

52
53
54
55
56
57
58
59
60
A deeper insight into the type of nitrogen species that become incorporated into samples
A-F can be obtained by the fitting analysis of the spectra in Fig. 5. We have intended
such an analysis under the assumption that all the spectral shapes can be well
reproduced by the contribution of three bands centred at 396.1 (species α), 399.3
(species β) and 400.7 (species β') eV. The results of the fitting analysis are reported in

1
2
3 Fig. 5. The fitting scheme used implies that around 396 eV there is only one type of
4 nitrogen species, while around 400 eV there is the contribution of two different bands. It
5 is important to note that this fitting scheme based on the presence of three bands
6 provides the minimum number of fitting bands with a similar width (i.e. between 1.7
7 and 1.4 eV) that would be common for the six analysed spectra. However, we must
8 stress that this analysis does not discard the presence of other possible species
9 characterized by BEs similar to those of the three bands resulting from the fitting
10 analysis.
11

12 The XPS analysis of the state of nitrogen in N-doped TiO₂ thin films has been widely
13 addressed in the recent literature on the subject,^{1, 8, 10-16, 32, 46-49} although no agreement
14 exists neither about the attribution of the detected species nor about the species which
15 is/are responsible for the visible light photoactivity of N-doped TiO₂. Of particular
16 interest is the recent paper by Asahi et al.⁴⁹ who based on first-principles calculations
17 using the projector argument wave method⁵⁰ has attributed the observed peaks in a
18 series of N-doped TiO₂ photocatalysts to N (395.7 eV), NO (398.1 eV) and NO₂ (399.8
19 eV) species. Nitrogen species with BEs around these values have been detected during
20 the oxidation of titanium nitride compounds^{51, 52} or by the nitrogen implantation in
21 titanium and other metal oxides.^{53, 54} Based on these previous works, we tentatively
22 ascribed the species detected in our films to nitride (396.3 eV) (i.e., nitrogen triple
23 bonded to titanium) and to nitrogen in a titanium oxinitride local environment (399.3 eV
24 and 400.7 eV) where nitrogen simultaneously bonds to oxygen and to titanium in a
25 defective lattice site (i.e., in a kind of Ti-N-O local structure). Within this scheme, a
26 different covalent character of the N-Ti bond would account for the differences in BE
27 between the two β species (e.g., structures of the type: Ti-N-O \cdots Ti or Ti-O-N \cdots Ti).
28 Basically, this tentative attribution assumes some kind of bonding between nitrogen and
29 oxygen for the species yielding the peaks at around 400 eV. In line with some previous
30 reports on this subject,¹¹ the latter attribution assumes that the nitrogen is also bonded to
31 titanium. The need of bonding to an electrophilic atom is, on the other hand, a
32 requirement because species like NO⁻, NO₂⁻ or NO₃⁻ where nitrogen is solely bonded to
33 oxygen atoms are characterized by BEs larger than 402 eV⁵⁵ and molecular nitrogen
34 species implanted in oxides are characterized by a BE of 403.4 eV.⁵⁴ In our case, the
35 attribution of the nitrogen species at around 400 eV to a nitrogen atom simultaneously
36 bonded to oxygen and titanium of the lattice was further sustained by the analysis of a
37 N-doped TiO₂ sample prepared by PECVD using TDEAT as precursor and a plasma of
38
39
40
41
42
43
44
45
46
47
48
49
50
51
52
53
54
55
56
57
58
59
60

1
2
3 pure oxygen. In that case only a N1s broad band at around 400 eV, with a N/Ti ratio of
4 0.01, could be detected even if no nitrogen was present in the plasma (see supporting
5 information S2). The fact that in the TDEAT precursor there are four nitrogen atoms
6 directly bonded to the titanium supports that after extensive oxidation of the precursor
7 during the plasma deposition process, some nitrogen may remain directly bonded to the
8 Ti although also interacting with the oxide ions of the lattice.
9

10 11 12 13 14 15 16 3.5. Photoactivity of N-doped thin films.

17 A first way of probing the photo-activity of titanium oxide thin films is by measuring
18 the wetting contact angle for samples exposed to illumination with UV, vis and/or
19 UV+vis light. As indicated in the introduction we will refer to this experiment as
20 *surface* photo-activity. Another way is by measuring the photo-catalytic activity of the
21 films.⁵⁶⁻⁵⁹ These experiments will be denoted here as *Schottky barrier driven* photo-
22 activity. In a recent publication on un-doped TiO₂²² we have pointed out that these two
23 tests are not equivalent and that they may yield different information about the photo-
24 activity of the studied systems. Here, we have tested the surface photo-activity of the
25 different films by measuring the evolution of the wetting angle when they are
26 illuminated with vis and UV+vis lights as a function of the irradiation time. *Schottky*
27 *barrier driven* photo-activity tests consist of measuring the photo-catalytic degradation
28 of methyl orange dye in an aqueous solution.
29

30 Fig. 6 shows four experiments taken as examples of the *surface* photo-activity
31 behaviour of the different thin films when they are illuminated, first with visible light
32 and then with UV light. The recovery of the wetting angle in the dark is also included.
33 The behaviour depicted by the REF thin film and sample E is typical of stoichiometric
34 TiO₂ surfaces and consists of the transformation of the surface of this material from
35 hydrophobic into super-hydrophilic when illuminated with UV light.⁶⁰ When the film is
36 left in the dark, it slowly recovers the initial wetting angle. These processes are very
37 affected by the topography of the surfaces and large variation in wetting angles can be
38 produced for nanostructured thin films in the form of fibres or similar nanostructures.⁶¹
39 In our case, a similar behaviour was also observed for samples C and D. The plots in the
40 right side of Fig. 7, depict the behaviour of samples A and F. Sample B also follows a
41 similar pattern. These plots are characterized by a partial and slow decrease in wetting
42 angle for about 30-40 °C when these thin films are illuminated with visible light and a
43 subsequent sharp decrease when the films are illuminated with UV+vis light. In the
44
45
46
47
48
49
50
51
52
53
54
55
56
57
58
59
60

1
2
3 dark, the films slightly recover the wetting angle reached upon visible light
4 illumination. A similar behaviour has been previously reported by us for N-doped TiO₂
5 and Ta₂O₅ thin films prepared by ion implantation^{23,29} or by other authors for thin films
6 prepared by magnetron sputtering.⁶² In other works from literature, complete
7 transformation into the superhydrophilic state of the surface of N-doped TiO₂ thin films
8 upon visible light irradiation has been also reported.⁶³
9
10
11
12
13

14
15 The *Schottky barrier driven* photo-activity of films A-F towards the degradation of the
16 methyl orange dye was analysed by illuminating with visible and with visible+UV light.
17 We observed that none of A-E films presented a detectable activity in the visible, while
18 samples A and B were active for photo-degradation of the dye only when they were
19 illuminated with UV+vis light, although this activity was smaller than that of the
20 reference sample. Meanwhile, thin films F were active with both visible and UV
21 irradiation. A comparison of the activity of the different films is reported in Fig. 7 for
22 illumination with UV+vis and vis lights. The lack of *Schottky barrier driven* photo-
23 activity in the visible for samples A-E is somehow contradictory with previous works in
24 literature reporting the visible photo-degradation of dye solutions with N-doped TiO₂
25 materials.^{1, 8, 32, 49, 56-59} Differences in experimental conditions, such as the use of
26 methylene blue (MB) as sacrificial dye in most of these previous works or the fact that
27 we are working with nanometric thin films and not with powders might be reasons for
28 this discrepancy. In fact, while the methyl orange solutions used in our case are stable
29 under visible light irradiation (but not under UV irradiation), MB solutions are not
30 stable either under UV or visible illumination. According to our experience, this and
31 other factors generally not considered explicitly in the experimental parts of the papers,
32 such as the control of both the concentration of oxygen and the temperature in the
33 reaction vessel during illumination or the inner vessel reflectivity in the blank
34 experiments are factors that, if not properly handled, may lead to flawed experiments and
35 misleading results (e.g., uncontrolled direct light degradation of the dye in the solution).
36
37
38
39
40
41
42
43
44
45
46
47
48
49
50
51
52
53

54 **4. Discusión**

55
56 The analysis of samples A-F has shown that they present different structures,
57 microstructures and compositions. XRD and Raman analysis of samples (cf. Figs. 2 and
58 3) have shown that only samples A and B present well defined peaks attributed to the
59
60

1
2
3 anatase structure. According to the Raman spectra in Fig. 3, samples D also present an
4 incipient crystallinity. Meanwhile, F samples consist of a mixture of the anatase and
5 rutile structures of TiO₂. The poor crystallinity of samples D must be related with the
6 [enhancement of ion bombardment effects during the preparation of the samples under](#)
7 [ECR conditions.](#)^{24, 25} Meanwhile, the amorphous character of samples E, even if
8 prepared at 523 K by PECVD, is likely related with the considerable reduction degree
9 of these samples and/or with the high concentration of Ti-N species incorporated into
10 [their](#) structure. On the other hand, comparison of the main peak of the Raman spectra of
11 the reference sample and those of samples A, B and F indicates that these N-doped thin
12 films present a considerable concentration of structural defects. We think that the
13 incorporation of nitrogen within the structure of these samples is contributing to this
14 effect.
15

16
17 The amount and chemical character of nitrogen incorporated in the structure of the films
18 was also different depending [on the sample](#). The concentration of nitrogen follows the
19 order E>D=C>B>A=F (cf. Table 1) a similar trend than for the ratio $\omega/(\beta + \beta')$ between
20 the different kinds of nitrogen species. It is important to remark that samples E,
21 characterized by the highest [absolute and relative concentrations](#) of [both](#) nitrogen and
22 species α , [respectively](#), present a high reduction degree. This result permits to establish
23 a link between the formation of Ti-N species of the α type and the reduction degree of
24 titanium oxide.
25

26
27 Species $\beta + \beta'$ are a majority in samples A, B and F, all of them prepared under mild
28 oxidant conditions and where, consequently, with little or no lattice reduction. Quite
29 interesting is that only these samples present *surface* photo-activity in the visible.
30 According to our tests, this means that species α with a BE around 396 eV (attributed to
31 Ti-N) would be inactive for the visible photo-activation of N-doped TiO₂ and that the
32 presence of species β and/or β' is a requirement for *surface* photo-activity in the visible.
33 Some hints in the recent literature on the subject^{12, 32, 48} agree with this behaviour of
34 samples A-F. This finding is in apparent contradiction with previous reports in literature
35 where the photo-activity of N-doped TiO₂ thin films has been associated with the
36 presence of species α ,^{1, 62} although in most cases the two species, α and β , have been
37 simultaneously detected. Without discarding other effects, a possibility [is that in many](#)
38 [previous experiments dealing with N-doped TiO₂ samples](#) the distribution of nitrogen
39 species is heterogeneous, so that the measured photo-activity in the visible responds
40 exclusively to those parts of the samples with a majority concentration of $\beta - \beta'$ species.
41
42
43
44
45
46
47
48
49
50
51
52
53
54
55
56
57
58
59
60

1
2
3 In powder materials this heterogeneity might correspond to a different distribution of
4 nitrogen species in the individual grains of the specimens. In addition, in thin films,
5 inhomogeneities in the depth distribution of nitrogen species might be an additional
6 factor modifying the visible photo-activity of samples.
7
8

9
10 It has been generally considered that visible photo-activity of N-doped TiO₂ is linked
11 with a shift in the position of the absorption edge.^{10, 11} Our results with samples A-F,
12 without completely contradicting this view, introduce some nuances which deserve a
13 specific consideration. Data in table 1 suggest a certain correlation between the
14 concentration of nitrogen in the sample and the magnitude of the shift in the absorption
15 edge. This means that those samples with a high concentration of the α species present a
16 maximum shift in the absorption edge. This finding precludes an automatic use of the
17 value of the absorption edge as a measurement of photo-activity since we have
18 demonstrated that this species does not contribute to the visible photo-activity of the
19 system. In this regard, it is worth noting that samples A, even presenting *surface* photo-
20 activity in the visible attributed to the incorporation of species β/β' in its structure (cf.
21 Fig. 5), do not present any significant shift of the absorption edge. This suggests that
22 other factors like lattice reduction or the presence of other defective sites associated to
23 nitrogen must contribute to the shift in the absorption edge. A similar description has
24 been proposed by Serpone et al^{11, 38} to account for the edge shift in N-doped TiO₂.
25
26

27
28 From the three samples, A, B and F, that present *surface* photo-activity in the visible,
29 only sample F presents *Schottky barrier driven* photo-activity. From the point of view
30 of XPS this sample is very similar to sample A, although structurally sample F consists
31 of a mixture of anatase and rutile and presents a shifted edge and some absorption band
32 in the visible (cf. Table 1). This result suggests that the development of local electronic
33 heterojunctions between zones consisting of N-doped anatase and N-doped rutile could
34 be a condition for the *Schottky barrier driven* photo-activity of this type of samples. It
35 could be also possible that in these samples a minority oxinitride phase, not detected in
36 the Raman spectrum, is the responsible for the observed photo-catalytic activity. At
37 present, more experimental and theoretical work is being carried out to ascertain these
38 hypotheses.
39
40

41
42 In any case, the photo-activity results found for samples A, B and F permits to establish
43 that wetting angle variation and photo-catalytic activity are two related but different
44 manifestations of the photo-activity of N-doped TiO₂. The terms *surface* and *Schottky*
45 *barrier driven* photo-activities used for convenience through all this manuscript deserve
46
47
48
49
50
51
52
53
54
55
56
57
58
59
60

1
2
3 now a justification. Photo-catalytic degradation of dye molecules is a complex process
4 implying the migration of photo-excited electrons and holes from the irradiated solid up
5 to its surface. The migration of UV induced photo-holes through the valence band of
6
7 TiO₂ is the rate controlling step of this process and is driven by the formation of a
8
9 Schottky barrier at the surface.^{10, 11, 64} A similar migration of photo-holes produced by
10
11 visible light should be expected in the case of N-doped TiO₂. However, such a
12
13 migration from the bulk would only be possible if the electronic states associated to
14
15 nitrogen forms a continuous band (or interband located between the valence and
16
17 conduction band of TiO₂^{8, 9}). Although we have to explore further the reasons why
18
19 samples F present *Schottky barrier driven* photo-activity, it is reasonable to think that
20
21 the formation of anatase/rutile heterojunctions could contribute to favor the migration of
22
23 photo-holes from the interior of the material up to its surface. In this regard, it is worthy
24
25 of mention a recent paper by Zhang et al.,⁶⁵ showing that, in TiO₂ powders consisting of
26
27 rutile grains covered by small anatase nanoparticles, the photo-catalytic reduction of
28
29 ethanol or water towards the formation of H₂ is enhanced with regard to a sample
30
31 consisting of pure anatase.

32 On the other hand, *surface* photo-activity, manifested as a change in the wetting angle
33
34 by visible irradiation of the N-TiO₂ thin films, would be a less strict process if just the
35
36 photo-holes generated at *the outmost surface layer(s)* intervene in the photo-induced
37
38 reaction. *Since the number of photo-holes required to induce the change in wetting*
39
40 *angle is expected to be much smaller than for a sustained photo-catalytic process, it is*
41
42 *reasonable to assume that just photo-excitation processes affecting the top most layer of*
43
44 *the sample may be enough to modify this surface property. Thus, although it seems that*
45
46 *in samples A and B there are no conditions for a Schottky barrier driven migration of*
47
48 *photoholes generated with visible light, surface photo-excitation processes seem to be*
49
50 *enough to induce the observed change in water contact angle.* A scheme in this sense
51
52 was proposed by us in a previous publication with N-doped TiO₂ samples prepared by
53
54 nitrogen implantation where we also explained why the wetting angle does not
55
56 necessarily yield the superhydrophobic state (i.e., wetting angle lower than 10°).²³

57 **5. Conclusions**

58 In this paper we have prepared N-doped TiO₂ thin films by PECVD and GAPVD. We
59
60 have been able to prepare samples that are amorphous (samples C and E), partially
amorphous (samples D), samples with the anatase structure (samples A and B) and

1
2
3 other set of samples (samples F) that consists of a mixture of anatase and rutile.
4
5 Samples D and, particularly, E were partially reduced and presented a relative high
6
7 absorption in the visible ($\lambda > 500$ nm) that is not attributed to the incorporation of
8
9 nitrogen within their structure.

10
11 Different nitrogen species have been detected in the samples by XPS. These species
12
13 have been tentatively attributed to Ti-N and Ti-N-O species. The first one is majority in
14
15 samples C-E and its formation in our films is associated with working conditions that
16
17 induce a certain reduction of the titanium oxide lattice (i.e., some hydrogen in the
18
19 plasma or deposition conditions where ion bombardment effects may have a
20
21 considerable importance). Under partially oxidant conditions as those used for the
22
23 preparation of samples A, B and F, Ti-N-O like species are majority. Samples A and B,
24
25 both containing relatively low concentration of species Ti-N-O did not present photo-
26
27 catalytic activity in the visible (i.e., *Schottky barrier driven* photo-activity) and were
28
29 less efficient for the photo-catalytic degradation of dye solutions under UV irradiation
30
31 than the reference anatase sample. By contrast, the wetting contact angle on its surface
32
33 decreased when irradiated with visible light (i.e., these samples presented visible
34
35 *surface* photo-activity). This suggests that this kind of nitrogen species is the
36
37 responsible of the visible photo-activity of N-doped TiO₂. It is also proposed that the
38
39 wide and sometimes contradictory set of results in the literature relating photo-activity
40
41 and type of nitrogen species can be the result of the heterogeneous distribution of the
42
43 Ti-N and Ti-N-O species within the samples, in such a way that active zones or grains
44
45 with the required type and concentration of nitrogen species are the sole responsible for
46
47 the visible activity of the whole specimen.

48
49 From our samples, only sample F presented both *surface* and *Schottky barrier driven*
50
51 photo-activities in the visible. This sample only had Ti-N-O like species incorporated in
52
53 its structure but consisted of a mixture of the anatase and rutile phases. This type of
54
55 samples also presented some absorption features in the visible and a shifted position of
56
57 the absorption edge. Further theoretical and experimental work is *being undertaken* to
58
59 ascertain all the *factors that are required* for *Schottky barrier driven* photo- activity with
60
61 visible light *in N-doped TiO₂ systems*.

6. Acknowledgments

We thank the Ministry of Science and Education of Spain (projects MAT 2007-65764/NAN2004-09317, and the CONSOLIDER INGENIO 2010-CSD2008-00023)

and the Junta de Andalucía (projects TEP2275 and P07-FQM-03298) for financial support. Part of this work has been carried out within the EU project NATAMA (contract nº 032583).

References

- 1.-R. Asahi, T. Morikawa, T. Ohwaki, K. Aoki, Y. Taga, *Science* 293, 269 (2001)
- 2.-S. Sakthivel, M. Janczarek, H. Kirsch, *J. Phys. Chem. B* 108, 19384 (2004)
- 3.-O. Diwald, T. L. Thompson, T. Zubkov, E. G. Goralski, S.D. Walck, J.T. Yates, *J. Phys. Chem. B*, 108, 6004 (2004)
- 4.-Y. Nosaka, M. Matsushita, J. Nasino, A. Y. Nosaka, *Sci. technol. Adv. Mater.* 6, 143 (2005)
- 5.-Y. Nakano, T. Morikawa, T. Ohwaki, Y. Taga, *Appl. Phys. Lett* 86, 132104 (2005)
- 6.-O. Diwald, T.L. Thompson, E.G. Goralski, S.D. Walck, J.T. Yates, *J. Phys. Chem. B* 108, 52 (2004)
- 7.-H.M. Yates, M.G. Nolan, D.W. Sheel, M.E. Pemble, *J. Photochem. Photobiol. A: Chemistry* 179, 223 (2006)
- 8.-S. Livraghi, M.C. Paganini, E. Giamello, A. Selloni, C.D. Valentin, G. Pacchioni, *J. Am. Chem. Soc.* 128, 15666 (2006)
- 9.-J.-Y. Lee, J. Park, J.-H. Cho, *Appl. Phys. Lett.* 87, 011904 (2005)
- 10.-T.L. Thompson, J.T. Yates, *Chem. Rev.* 106, 4428 (2006)
- 11.-A.V. Emeline, V.N. Kuznetsov, V.K. Rybchuk, N. Serpone, *Int. J. Photoener.* (2008) Art. ID 258394
- 12.-X. Chen, C. Burda, *J. Phys. Chem. B* 108, 15446 (2004)
- 13.-S. Sato, R. Nakamura, S. Abe, *Appl. Catal. A-Gen.* 284, 131 (2005)
- 14.-C.S. Gopinath, *J. Phys. Chem. B* 110, 7079 (2006)
- 15.-R. Nakamura, T. Tanaka, Y. Nakato, *J. Phys. Chem. B* 108, 10617 (2004)
- 16.-R.P. Vitiello, J.M. Macak, A. Ghicov, H. Tsuchiya, L.F.P. Dick, P. Schmuki, *Electrochem. Commun.* 8, 544 (2006)
- 17.-J.M. Mwabora, T. Lindgren, E. Avendano, T.F. Jaramillo, J. Lu, S.E. Lindquist, C.G. Granqvist *J. Phys. Chem. B* 108, 20193 (2004)
- 18.-H. Irie, S. Washizuka, Y. Watanabe, T. Kako, K. Hashimoto, *J. Electrochem. Soc.* 152, E351 (2005)
- 19.-M.-Ch. Yang, T.-S. Yang, M.-Sh. Wong, *Thin Sol. Films* 469/470, 1 (2004)
- 20.- T.-S. Yang, M.-Ch. Yang, Ch.-B. Shiu, W.-K. Chang, M.-Sh. Wong, *Appl. Surf. Sci.* 252, 3729 (2006)
- 21.-M. Maeda, T. Watanabe, *J. Electrochem. Soc.* 153, C186 (2006)
- 22.-V. Rico, P. Romero, J.L. Hueso, J.P. Espinós, A.R. González-Elípe, *Catal. Today*, in press in the web
- 23.- A. Borrás, C. López, V. Rico, F. Gracia, A. R. González-Elípe, E. Richter, G. Battiston, R. Gerbasi, N. McSparran, G. Sauthier, E. György, and A. Figueras, *J. Phys. Chem. C*; 111, 1801 (2007)
- 24.- A. Borrás, J. Cotrino, A. R. González-Elípe, *J. Electrochem. Soc.*, 154, 152 (2007)
- 25.- F. Gracia, J.P. Holgado, A.R. González-Elípe, *Langmuir* 20, 1688 (2004)

- 1
2
3 26.- D. Korzec, F. Werner, R. Winter, J. Engemann, *Plasm Sources Sci. Technol.* **6**, 216
4 (1996)
5 27.- A.C. van Popta, J. Cheng, J.C.Sit, M.J. Brett, *J. Appl. Phys.* 102, 013517 (2007)
6 28.- M. M. Hawkeye, M.J. Brett, *J. Vac. Sci. Technol. A* 25, 1317 (2007)
7 29.- V. Rico, A. Borrás, F. Yubero, J. P. Espinós, F. Frutos, A. R. González-Elipe J.
8 *Phys. Chem. C* in press
9 30.- J.A.Dood, S.J.Lipson, D.J.Flanagan, W.A.M.Blumberg, J.C.Person, B.O.Green, J.
10 *Chem.Phys.* **94**, 4301 (1991)
11 30.- T. Ohsaka, F. Izumi, Y. Fujiki, *J. Raman Spectrosc.*, Vol. 7, NO 6,1978
12 31.- J. Zhang, M. Li, Z. Feng, J. Chen, *Can Li, J. Phys. Chem. B* 110, 927 (2006)
13 32.- Y. Cong, J. Zhang, F. Chen, M. Anpo, *J. Phys. Chem. C* 111, 6976 (2007)
14 33.-A.I. Kontos, A. G. Kontos, D.S. Tsoukleris, G.D. Vlachos, P. Faralas, *Thin Soil.*
15 *Films*, 515, 7370 (2007)
16 34.- A.I. Kontos, A. G. Kontos, Y.S. Raptis, P. Faralas, *Phys. Stat. Soil.* 2, 83 (2008) 83
17 35.- J.C. Parker and R.W. Siegel, *Appl. Phys. Lett.* **57**, **943** (1990)
18 36.- E. Gyorgy, A. Pérez del Pino, P. Serra, J.L. Morenza, *Appl. Surf. Sci.* 186 (2002)
19 130
20 37.- M. Bernard, A. Deneuve, O. Thomas, P. Gergaud, P. Standstrom, J. Birch, *Thin*
21 *Sol. Films* 380 (2002) 252
22 36.- N. Martin, A. Besnard, F. Sthal, F. Vaz, C. Nouveau, *Appl. Phys. Lett.* 93, 064102
23 (2008)
24 37.- N. Serpone, D. Lawless, R. Khairutdinov, *J. Phys. Chem.* 99, 16646 (1995)
25 38.- N. Vyacheslav, N. Kuznetsov, N. Serpone, *J. Phys. Chem. B* 110, 25203 (2006)
26 39.- T. Umebayashi, T. Yamaki, H. Itoh, K. Asai, *Appl. Phys. Lett.* 81, 554 (2002)
27 40.- Z. Lei, G. Ma, M. Liu, W. You, H. Yan, G. Wu, T. Takata, M. Hara, K. Domen, C.
28 Li, *J. Catal.* 237, 322 (2006)
29 41.- B. Liu, L. Wen, X. Zhao, *Solar Energy Mater.&Solara cells* 92, 1 (2008)
30 42.- Z. lin, A. Orlov, R.M. Lambert, M.C. Payne, *J. Phys. Chem. B*, 109, 20948 (2005)
31 43.- E.L. Bullock, L. Patthey, S.G. Steinemann, *Surf. Sci.* 532/534, 504 (1996)
32 44.- A.R.González-Elipe, J.P.Espinós, A.Fernández, G.Munuera, *Appl. Surf. Science*, 45,
33 103 (1990)
34 45.- D. Leinen, A. Fernández, J.P. Espinós, A.R. González-Elipe, *Applied Physics A*, 63,
35 237 (1996)
36 46.- Y. Zhao, X. Qiu, C. Burda, *J. Phys. Chem.* 20, 2629 (2008).
37 47.- S. Clouser, A.C.S. Samia, E. Navok, J. Alred, C. Burda, *Top. Catal.* 47, 42 (2008)
38 48.- X. Qiu, Y. Zhao, C. Burda, *Adv. Mater.* 19, 3995 (2007)
39 49.- R. Asahi, T. Morikawa, H. Hazama, M. Matsubara, *J. Phys.: Condens. Matter* 20,
40 064227 (2008)
41 50.- P.E. Blochl, *Phys. Rev. B* 50, 17953 (1994)
42 51.- R. Lahoz, J.P. Espinós, G.F. de la Fuente, A.R. González-Elipe, *Surf. Coat.*
43 *Technol.* 2002, 1486 (2008)
44 52.- F. Esaka, K. Furuya, H. Shimada, M. Imamura, N. Matsubayashi, H. Sato, A.
45 Nishijima, A. Kawana, H. Ichimura, T. Kikuchi, *J. Vac. Sci. technol. A* 15, 2521 (1997)
46 53.- I. Bertoti, R. Kelly, M. Mohai, A. Toth, *Surf. Interf. Anal.* 19, 291 (1992)
47 54.- A. Barranco, J.P. Holgado, F. Yubero, J.P. Espinós, A. Martín, A.R. González-
48 Elipe, *J. Vac. Sci. technol.* 19, 1024 (2001)
49 55.- C.D. Batich, D.S. Donald, *J Am Chem Soc* 106, 2758 (1984)
50 56.- Y. Zhao, X. Qiu, C. Bruda, *Chem. Mater.* 20, 2629 (2008)
51 57.- M. Okada, Y. Yamada, P. Jin, M. Tazawa, K. Yoshimura, *Appl. Surf. Sci.* 254, 156
52 (2007)
53
54
55
56
57
58
59
60

- 1
2
3 58.- T-S. Yang, M.Ch. Yang, Ch.-B. Shiu, W.-K. Chang, M-Sh. Wong, Appl. Surf. Sci.
4 252, 3729 (2006)
5
6 59.- M-Ch. Yang, T.-S. Yang, M.-Sh. Wong, Thin Sol. Films, 469/470, 1 (2004)
7
8 60.- R. Wang, K. Hashimoto, A. Fujishima, M. Chikuni, E. Kojima, A.Kitamura, M.
9 Shimohigoshi, T. Watanabe, Nature 388, 431 (1997)
10
11 61.- A. Borrás, A. Barranco, A.R. González-Elipe, Langmuir 24, 8021 (2008)
12
13 62.- Q. Li, J.-K. Shang, J. Am. Chem. Soc. 91, 3167 (2008)
14
15 63.- J. Premkumar, Chem. Mater. 16, 3980 (2004)
16
17 64.-O. Carp, C.L. Huisman, A. Reller, Prog. Sol. State Chem. 32, 33 (2004)
18
19 65.-J. Zhang, Q. Xu, Z.Feng, M. Li, C. Li, Angew. Chem. Int. Ed. 47, 1766 (2008)
20
21
22
23
24

25 *Table 1.- Summary of main properties of samples*

26

PARAMETER OF SYNTHESIS				STRUCTURAL AND OPTICAL PROPERTIES		
Sample	T(K)	Plasma composition (N ₂ %, O ₂ %, H ₂ %)	Pressure (Torr)	Structure ¹ and crystal size (nm)	Absorption edge	N/Ti
A	523	(17,83,0)	4·10 ⁻³	A (84.2)	3.14 eV	0.01
B	523	(88,12,0)	4·10 ⁻³	A (85.0)	2.8 eV	0.04
C	298	(88,12,0)	4·10 ⁻³	Amor.	3.32 eV	0.11
D	523	(65,12,23)	4·10 ⁻³	Amor.	2.75 eV	0.11
E	523	(88,12,0)	4·10 ⁻⁴	Amor.	2.4 eV	0.24
F	673	PVD	10 ⁻⁴	A(22.6)+ R(9.0)	2,92 eV	0,01
REF	523	(0,100,0)	4·10 ⁻³	A (89.2)	3.22 eV	0

27
28
29
30
31
32
33
34
35
36
37
38
39
40
41
42
43
44
45
46
47
48
49

50
51 1) A: anatase; R: rutile; amor. amorphous
52
53
54
55
56
57

58 **Figure captions**

59
60 Scheme 1.- Representation of the structure of the TTIP and TDEAT precursors of Ti used for the PECVD of N-doped TiO₂ thin films

1
2
3 Fig. 1.- Cross section views of thin films A-F and that of the REF sample. Sample E has
4 a microstructure very similar to that of sample C.
5

6 Fig. 2.- XRD of samples A-F and that of the REF sample included for comparison.
7

8 Peaks due to the anatase and rutile phases are indicated in the form of patterns.
9

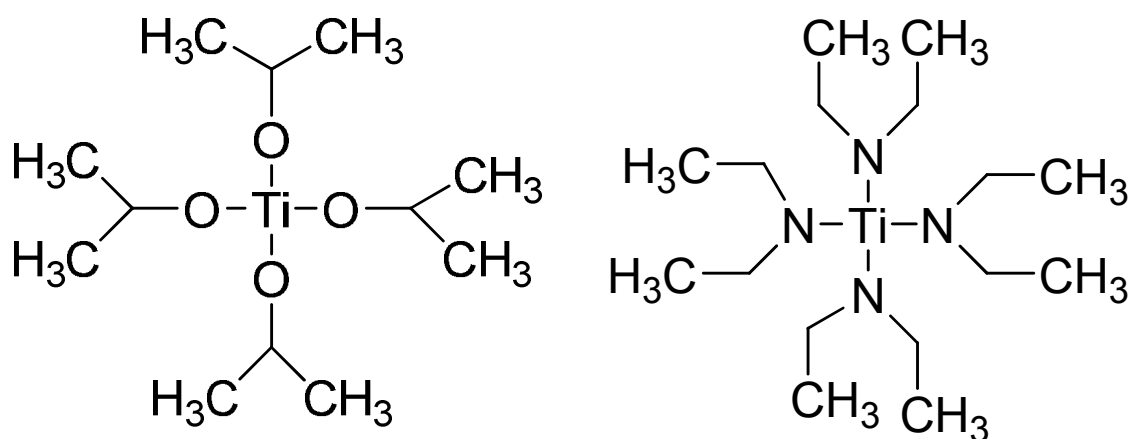
10 Figure 3.- (Top) Raman spectra in the zone between 200 and 800 cm^{-1} for samples A-F
11 compared with that of the reference anatase sample; the peaks attributed to the rutile
12 phase are indicated. (Bottom) Raman spectra in the zone of the main peak of anatase at
13 around 150 cm^{-1} .
14
15

16 Fig. 4.-UV-vis absorption spectra of samples A-F compared with that of the reference
17 thin film. The asterisk in some of the plots indicates the presence of a specific
18 absorption feature.
19
20
21

22 Figure 5.- N1s fitted photoemission spectra of samples A-F
23

24 Figure 6.- Evolution of the wetting angle for the REF and E thin films (left) and
25 samples A and F (right) subjected sequentially to illumination with visible, UV+vis and
26 then left in the dark. The curves are plotted to guide the eyes.
27
28

29 Figure 7.- Evolution of the concentration of methyl orange dye in an illuminated
30 solution of this molecule in the presence of the thin films. Curves corresponding to
31 experiments with UV+vis (left) and vis (right) illumination are reported. The curves
32 upon UV+vis illumination have been corrected by the curve of a solution of the dye in
33 the presence of a bare substrate of Si without thin film.
34
35
36
37
38
39
40
41
42
43
44
45
46
47
48
49
50
51
52
53
54
55
56
57
58
59
60



Scheme 1.- Representation of the structure of the TTIP and TDEAT precursors of Ti used for the PECVD of N-doped TiO₂ thin films

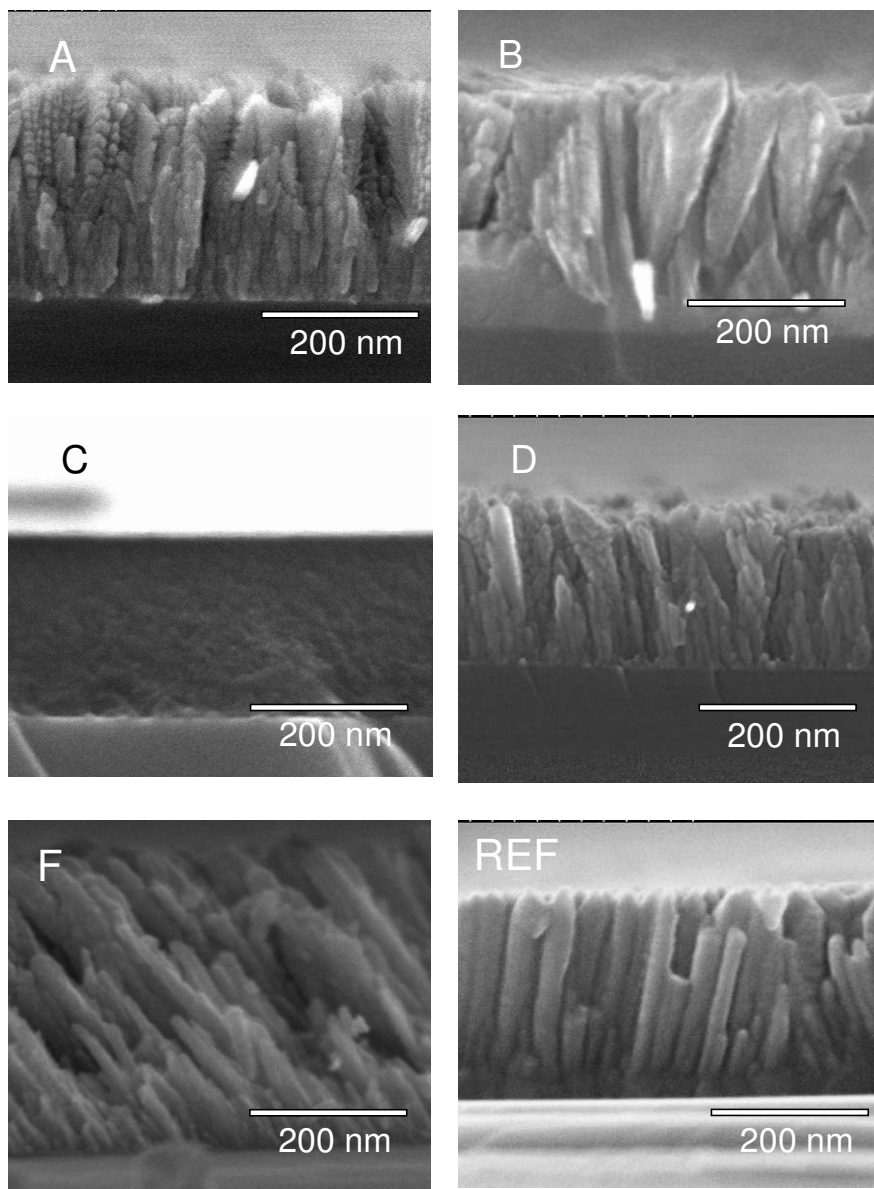


Fig. 1.- Cross section views of thin films A-F and that of the REF sample. Sample E has a microstructure very similar to that of sample C.

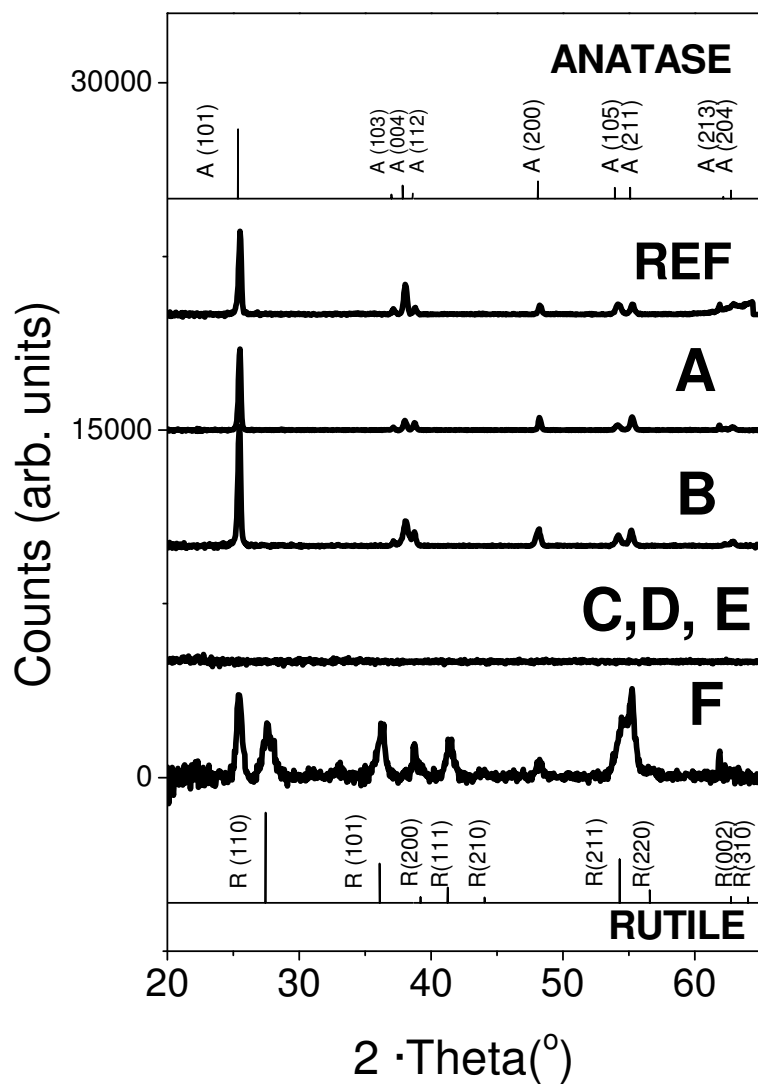


Fig. 2.- XRD of samples A-F and that of the REF sample included for comparison. Peaks due to the anatase and rutile phases are indicated in the form of patterns.

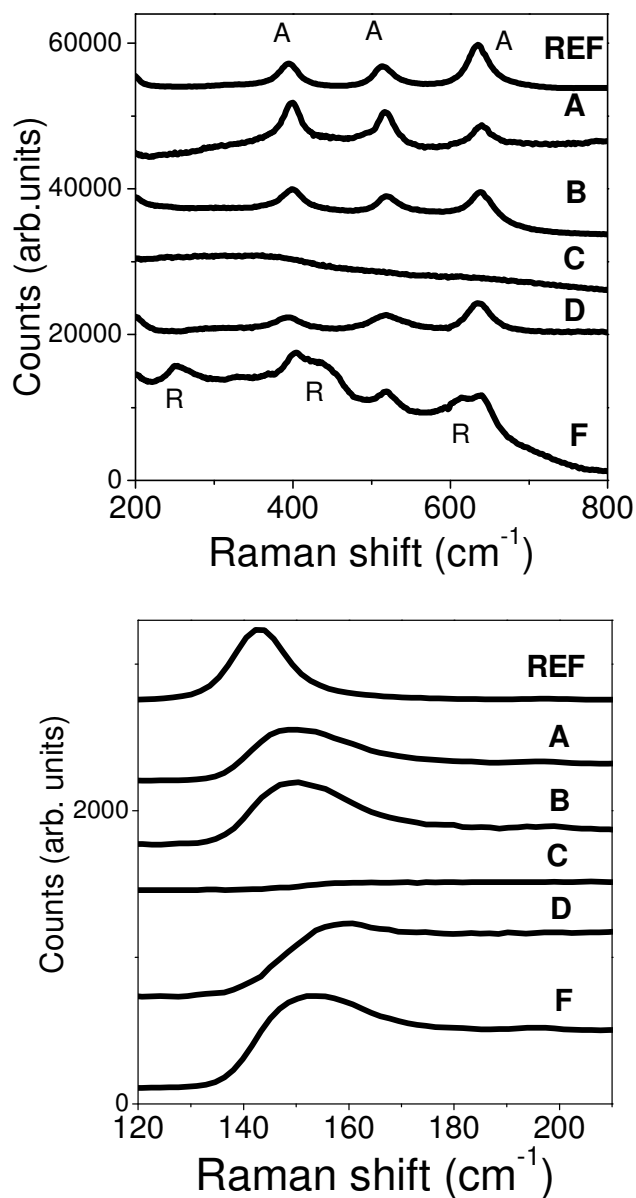


Figure 3.- (Top) Raman spectra in the zone between 200 and 800 cm⁻¹ for samples A-F compared with that of the reference anatase sample; the peaks attributed to the rutile phase are indicated. (Bottom) Raman spectra in the zone of the main peak of anatase at around 150 cm⁻¹.

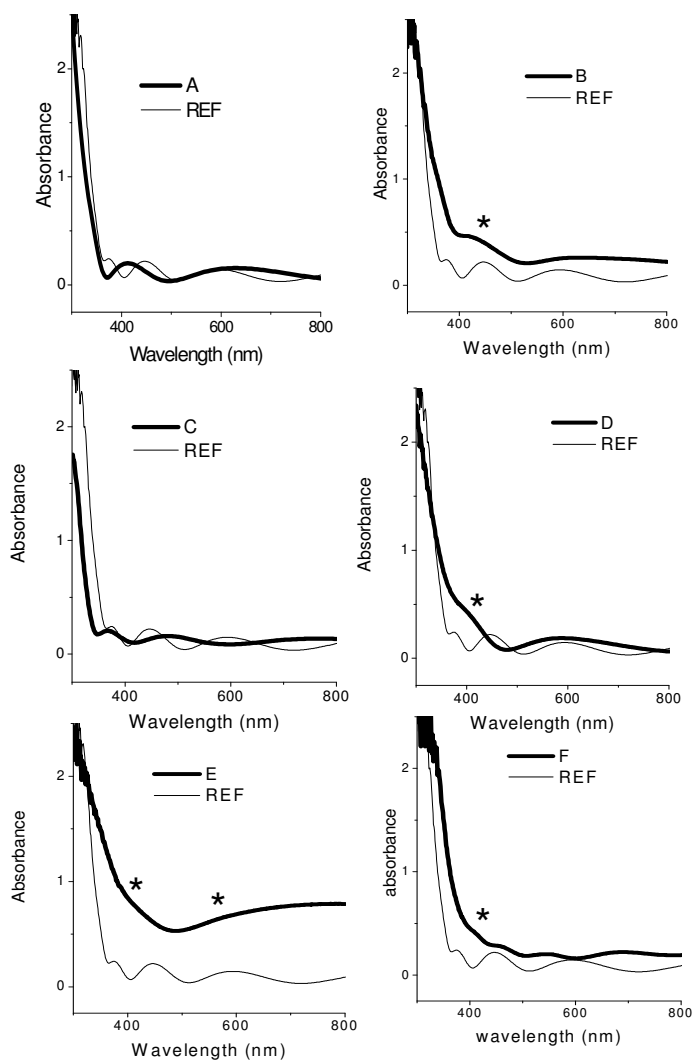


Fig. 4.-UV-vis absorption spectra of samples A-F compared with that of the reference thin film. The asterisk in some of the plots indicates the presence of a specific absorption feature.

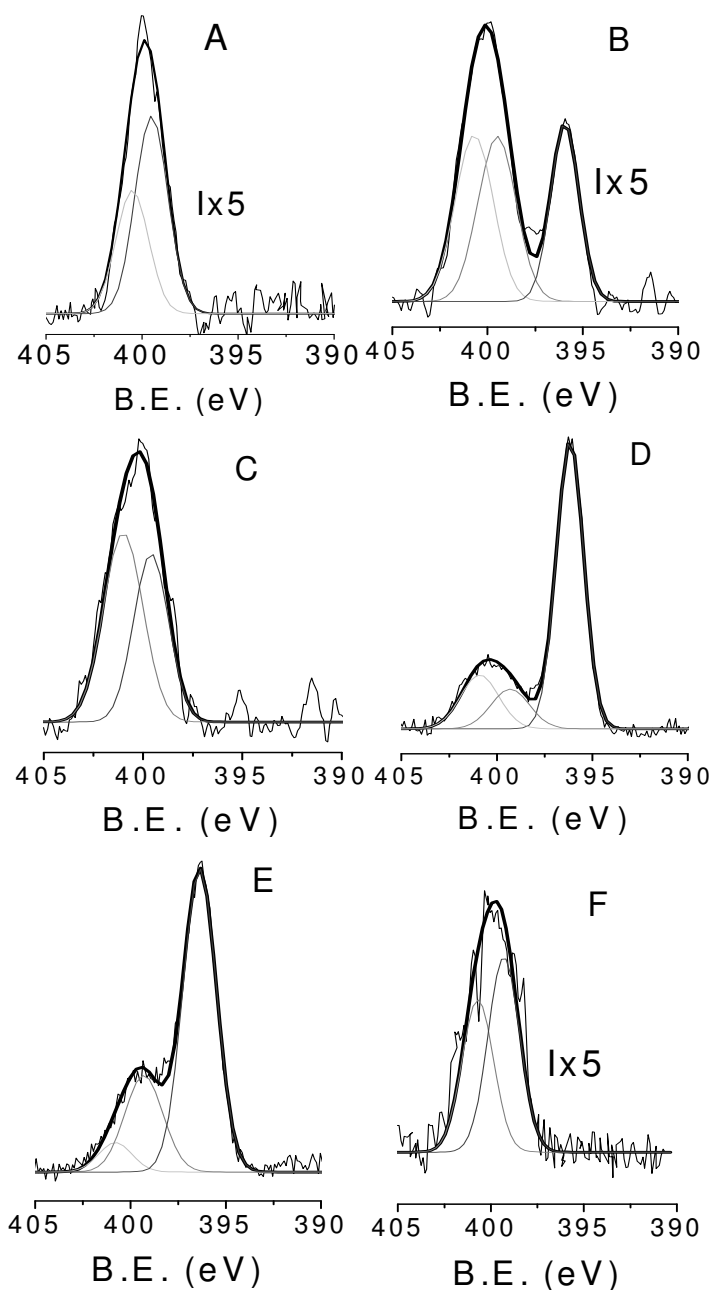


Figure 5.- N1s fitted photoemission spectra of samples A-F

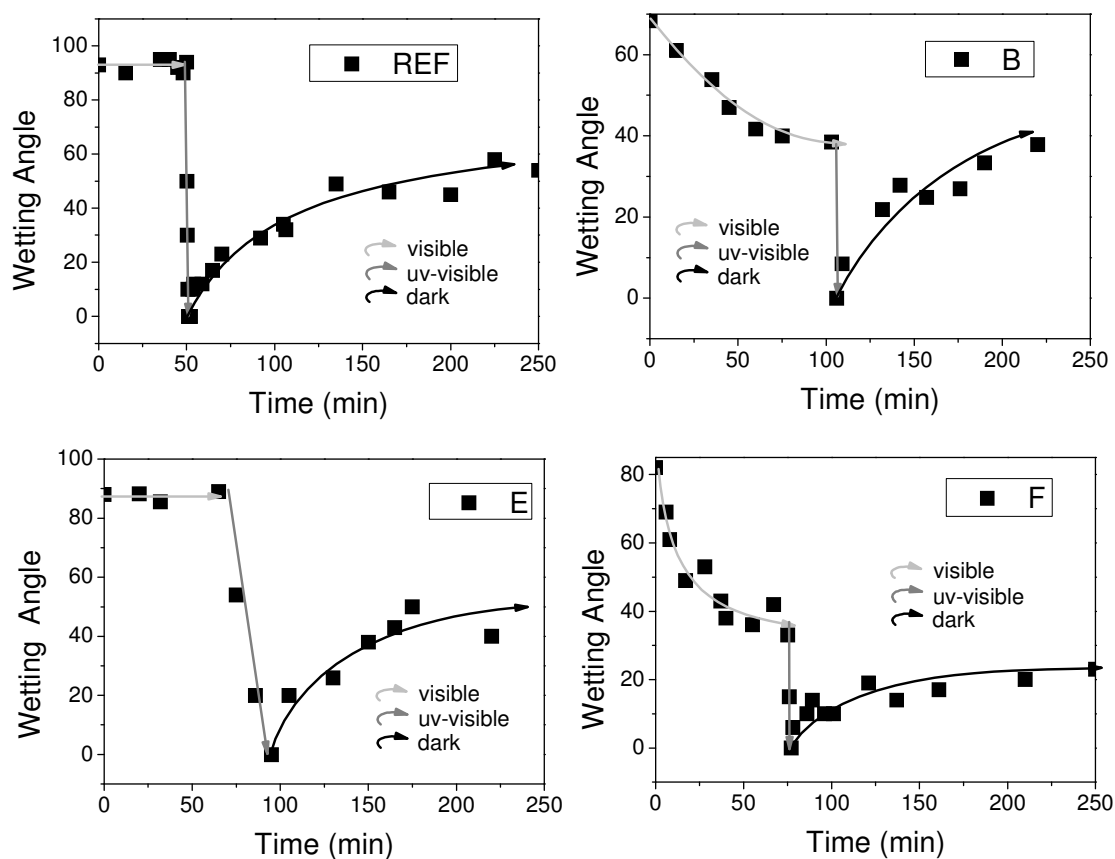


Figure 6.- Evolution of the wetting angle for the REF and E thin films (left) and samples A and F (right) subjected sequentially to illumination with visible, UV+vis and then left in the dark. The curves are plotted to guide the eyes.

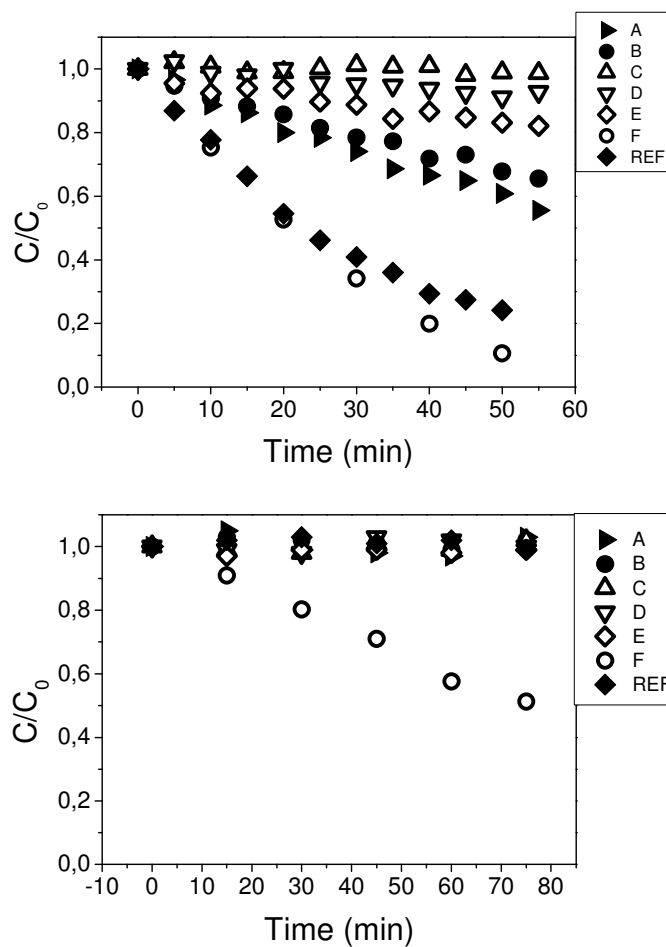


Figure 7.- Evolution of the concentration of methyl orange dye in an illuminated solution of this molecule in the presence of the thin films. Curves corresponding to experiments with UV+vis (top) and visible (bottom) illumination are reported. The curves upon UV+vis illumination have been corrected by the curve of a solution of the dye in the presence of a bare substrate of Si without thin film.